Iceberg calving during transition from grounded to floating ice: Columbia Glacier, Alaska

Fabian Walter,[1] Shad O'Neel,[2] Daniel McNamara,[3] W. T. Pfeffer,[4] Jeremy N. Bassis,[5] and Helen Amanda Fricker[1]

Received 16 March 2010; revised 7 May 2010; accepted 20 May 2010; published 7 August 2010.

[1] The terminus of Columbia Glacier, Alaska, unexpectedly became ungrounded in 2007 during its prolonged retreat. Visual observations showed that calving changed from a steady release of low-volume bergs, to episodic flow-perpendicular rifting, propagation, and release of very large icebergs - a style reminiscent of calving from ice shelves. Here, we compare passive seismic and photographic observations through this transition to examine changes in calving. Mechanical changes accompany the visible changes in calving style post flotation: generation of seismic energy during calving is substantially reduced. We propose this is partly due to changes in source processes. **Citation:** Walter, F., S. O'Neel, D. McNamara, W. T. Pfeffer, J. N. Bassis, and H. A. Fricker (2010), Iceberg calving during transition from grounded to floating ice: Columbia Glacier, Alaska, *Geophys. Res. Lett.*, *37*, L15501, doi:10.1029/2010GL043201.

1. Introduction

[2] Iceberg calving accounts for nearly 50% of the mass loss for both the Greenland and Antarctic ice sheets, [e.g., *van den Broeke et al.*, 2009; *Rignot et al.*, 2008]. Dominating eustatic sea-level rise, marine-terminating glaciers and ice-caps are susceptible to dynamic instabilities and calving mass can dominate mass loss terms [*Meier et al.*, 2007]. However, our understanding of calving is limited and calving is not well represented in models of ice sheets and glaciers. Passive seismic energy released during calving is an easily distinguishable signal that provides an innovative means to resolve mechanical processes [*Qamar*, 1988; *O'Neel et al.*, 2007]. Calving-related seismicity represents similar mechanical processes in temperate glaciers and polar ice sheet outlets [*O'Neel et al.*, 2007; *Amundson et al.*, 2008]. Although source mechanisms for emergent, narrow-band (1–3 Hz) and long-duration (up to hundreds of seconds) calving seismicity have not been established, resonance in water-filled cracks during calving failure [e.g., *O'Neel and Pfeffer*, 2007], as well as avalanching [*Amundson et al.*, 2010] have been proposed. Furthermore, these time and frequency domain properties allow batch separation of calving-related seismicity from the complete seismic record, which also includes high-frequency (above 5 Hz) signals associated with fracturing and surface crevassing [*Neave and Savage*, 1970; *Walter et al.*, 2009]. These seismic events often accompany iceberg calving, but can also occur independently of it.

[3] Columbia Glacier (Figure 1) began its rapid retreat ca. 1982. Elevated calving flux (≤7 km^3/yr), rapid surface velocities (≤30 m/d) and extreme thinning (≤450 m) [*O'Neel et al.*, 2005] have accompanied the 17+ km length change. As the glacier retreated through a constriction between Kadin and Great Nunatak Peaks (Figure 1), its terminus stabilized for several years, although thinning and fast flow continued. The constriction is associated with a basal over-deepening extending ~500 m below sea level. Once retreat progressed upstream of the constriction, the width of the calving front increased by approximately a factor of 3 (it currently exceeds 7 km in arc length). As the terminus cleared the over-deepened region, quasi-periodic, short-term (~2 week) ~500 m advance/retreat cycles began, and floating conditions developed. We estimate that ~2 km (centerline length) of the terminus region has been floating since mid-summer 2007 (Figure 1 and Animation S1 of the auxiliary material).[6]

[4] Here we use broadband seismic observations and time-lapse images collected in 2004–2005 and 2008–2009 to identify and interpret changes in calving dynamics during the transition from grounded to floating.

2. Instrumentation and Data Acquisition

[5] Since June 2004, at least one time-lapse camera has been deployed on the Great Nunatak side of the terminus and programmed to acquire a minimum of 4 images per day. Terminus retreat required us to move cameras on a nearly annual basis, and power failures and memory constraints have limited data acquisition. Nevertheless, an excellent piece-wise continuous record exists through the grounded-floating transition.

[6] We acquired broadband seismic data at the same location (station BBB; Figure 1) over two separate periods: June 2004 to September 2005 and June 2008 to present (January 2010). Both deployments used a Guralp 40T broadband seismometer. Instrumentation details can be found in the auxiliary material.

3. Data Analysis

[7] We used two complementary seismic analyses: (1) construction of a catalog of isolated seismic events related to calving; and (2) analysis of the seismic background noise.

[1]Institute of Geophysics and Planetary Physics, University of California, San Diego, La Jolla, California, USA.
[2]U.S. Geological Survey, Anchorage, Alaska, USA.
[3]U.S. Geological Survey, Golden, Colorado, USA.
[4]Institute of Arctic and Alpine Research, University of Colorado at Boulder, Boulder, Colorado, USA.
[5]Department of Geological Sciences, University of Michigan, Ann Arbor, Michigan, USA.

0094-8276/10/2010GL043201

[6]Auxiliary materials are available in the HTML. doi:10.1029/2010GL043201.

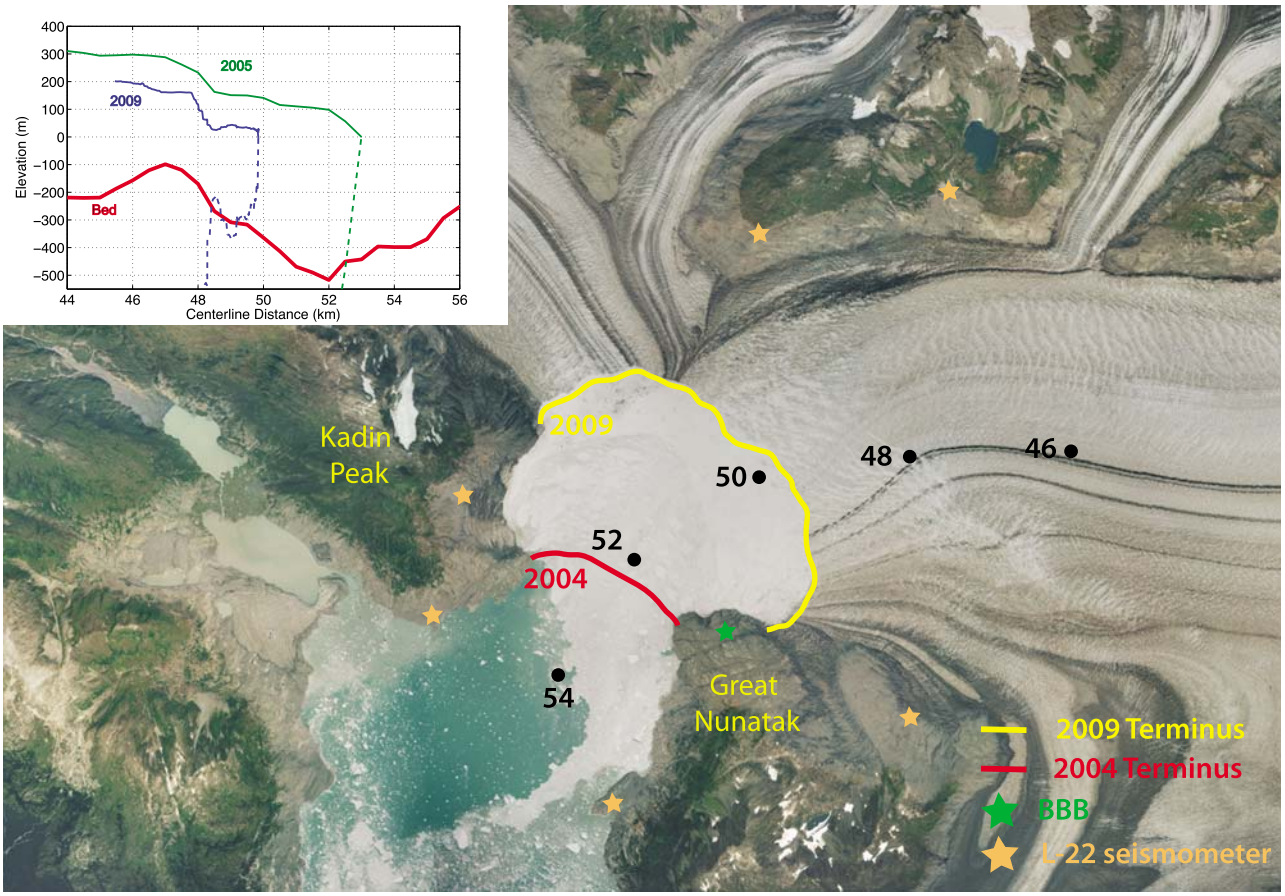

Figure 1. Overview image of Columbia Glacier, acquired 27 August 2009. The location of the 2004 terminus position is shown in red, and the green star marks the location of the broadband seismometer BBB. Orange stars represent short-period seismometers deployed during 2004–05 that all recorded 1–3 Hz energy related to calving. The Kadin-Great Nunatak gap described in the text refers to the constriction in the channel near the location of the 2004 terminus. The inset gives the centerline geometry of the glacier during 2005 (green) and 2009 (blue), following a coordinate system established by *Meier and Post* [1987]. Downstream of 54 km bathymetry is known from boat-based observations. Bed topography upstream of this location is modeled with continuity [*O'Neel et al.*, 2005]. Surface topography is extracted along the same coordinate system from orthorectified vertical photography. Dashed lines indicate the glacier base assuming hydrostatic equilibrium, demonstrating that the glacier was grounded in 2004. For 2009 this depicts a 1.6 km long floating tongue.

[8] For approach 1, we used frequency-domain event detection methods (Text S1), which isolate emergent, narrowband (peaked at 1–3 Hz) transients [*O'Neel et al.*, 2007]. Data gaps required corrections to remove detection time bias associated with an incomplete record. By summing detection durations over all available complete hour-long intervals, a direct comparison between deployments was possible. We only included recording times during which the station was recording in both deployments, assuring that differences in detection statistics were not attributed to data gaps.

[9] We removed detections of known tectonic earthquakes >ML 1.5 as documented by the Alaska Earthquake Information Center (http://www.aeic.alaska.edu/html_docs/db2catalog.html). To quantify the size of calving events, detection duration was recorded for each event [*Qamar*, 1988; *O'Neel et al.*, 2007]. We also examined high frequency fracture seismicity [*Walter et al.*, 2009].

[10] Approach 2 computed the background noise spectrum using probability density functions of power spectral density (PSD-PDF's) [*McNamara and Buland*, 2004]. The PSD-PDF evaluates spectra in moving time windows, normalized to provide estimates of seismic power as a function of frequency. For times comprised of many such windows, individual PSDs form an empirical PDF that characterizes seismic power and its variability as a function of frequency. The PSD-PDF method facilitates analysis of subtle time-spectral variations by providing statistical measures of power and frequency evolution. This quantifies seismic sources with a high occurrence probability, but weak amplitude, such as ocean waves and iceberg calving. In contrast, less frequent, high energy sources like earthquakes have a low occurrence probability, even though they produce high power PSD's in frequency ranges of interest.

4. Results

4.1. Time-Lapse Photography

[11] Our photographs show that floating iceberg debris thickened significantly since 2005. During 2008–2009 the debris was strong and thick enough to support a deep snowpack, which likely aided preservation of the floating ice tongue [*Amundson et al.*, 2010]. Both visual observations and

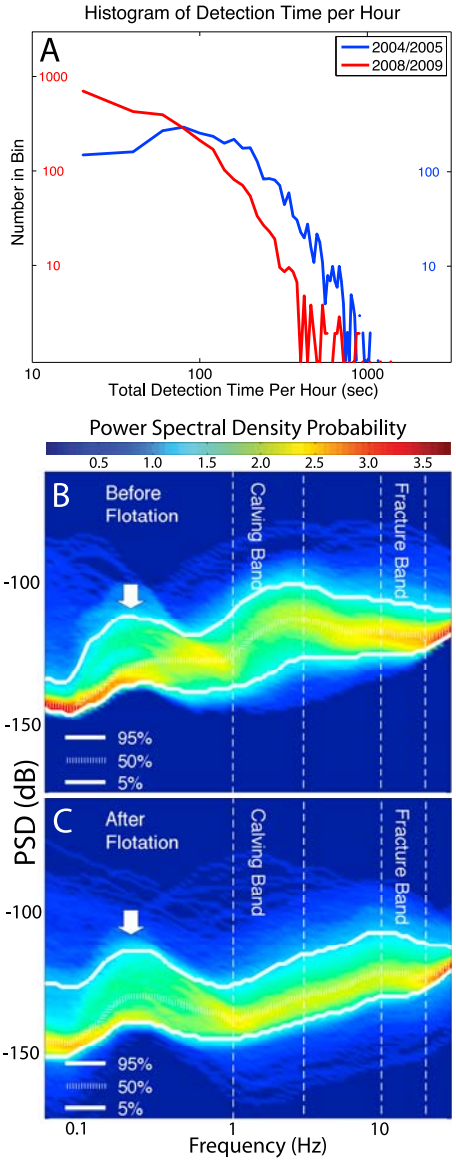

Figure 2. (a) Histograms of hourly detection time of calving seismicity for 2004–2005 and 2008–2009, before and after terminus flotation, respectively. Bin width is 20 seconds. (b and c) Probability density functions of power spectral density (PSD-PDF) for the continuous seismic record from station BBB near Columbia Glacier's terminus, acquired before (Figure 2b) and after (Figure 2c) terminus flotation, respectively. The white arrow marks the secondary microseism peak.

time-lapse photography document several interrelated changes at the terminus since flotation. The most noticeable change was a transition to infrequent, and much larger events (affecting over 30% of the terminus arc length) compared to frequent small-to-medium-sized events observed under grounded conditions. While the duration of the largest events remained relatively constant through the grounded-floating transition, the ice volume discharged per event increased substantially, perhaps by an order of magnitude. Development of large (>50% of glacier width), flow-perpendicular rifts in the terminus region (Figure S1) accompanied this change in calving style. In contrast to nearly instantaneous fracture and failure during grounded conditions, rifting proceeds over days to weeks as propagation occurs, and ultimately discharges a large berg. Rifts at distances of less than an ice thickness from the terminus isolate slabs, which slowly rotate forward as they detach (Figures S1a and S2b). In other instances where flow-perpendicular rifts are located further upstream from the terminus, the region in front of the rift calves by sudden, nearly *in situ* disintegration (Figures S1e and S1f). The calving of intact tabular icebergs has not been observed.

4.2. Seismic Approach

4.2.1. Changes in 1–3 Hz Calving Detection

[12] The event catalogs for each deployment show a shift towards less frequent calving-related seismicity: in 2004–2005, 4.74% of the total recording time was composed of 1–3 Hz detections; in 2008–2009, this number decreases by over a factor of 3 to 1.35%. In order to demonstrate the shift, detection durations were partitioned into 20-second bins and normalized by total population. Figure 2a shows results for detections on the z-component. Like the decrease in total detection time, the 2008–2009 data contain more quiet hours (less than 100 seconds detection time per hour) than the 2004–2005 data. Active hours (more than 100 seconds detection time per hour) were more abundant when the terminus was grounded. Hours with high detection times (500–1000 seconds) are present in both data sets.

4.2.2. Changes in Power Spectral Density

[13] Figures 2b and 2c also show the PSD-PDF's of the 2004–2005 and 2008–2009 data sets, respectively. Instrument response transfer functions are deconvolved allowing direct comparison of absolute ground motion between the two experiments. The 5th, 50th and 95th percentiles of the PDF distribution are shown and display three peaks. The prominent peak between 0.125 and 0.25 Hz is known as the Secondary microseism and is clearly observed in both data sets. This feature is observed at nearly all global seismic stations and is generated by ocean wave action at nearby coastlines, and in the deep ocean [*Longuet-Higgins*, 1950; *Aster et al.*, 2008]. The larger peak between 1 and 5 Hz lies within the calving seismicity band [*O'Neel et al.*, 2007] and exists only in the 2004–2005 record. Peaks in the 95 percentile and the median probability curves mark the frequency of maximum power. In 2008–2009, 1–5 Hz energy is absent suggesting a significant change in the calving dynamics. The 1–5 Hz peak is characteristic of the tidewater glacier environment, and its disappearance indicates a decrease in seismicity related to calving during the second deployment when the terminus was floating.

[14] A third peak at 10 Hz, with lower amplitude and probability, is observed in the 2008–2009 data set. As the 1–5 Hz peak masks this smaller peak in 2004–2005, it is difficult to say if this peak emerged between the two field deployments or if it is present in both data sets. Its origin may represent a relative increase in englacial fracturing [*O'Neel et al.*, 2007], local earthquakes or scraping of icebergs in the proglacial debris [*MacAyeal et al.*, 2008].

4.3. Change in Seismic Signature of Calving

[15] Mirroring the decrease in 1–3 Hz calving detections, the total number of 10–20 Hz fracturing detections decreased from 2.52% to 1.21% of the total recording time through the transition from grounded terminus to floating. To investigate

energy partitioning between the two frequency bands (1–3 Hz and 10–20 Hz) during calving events, we calculated the pseudo-energy by integrating the square of the vertical seismogram in both frequency bands, evaluating the pseudo-energy ratio between the two pass bands after removing extreme outliers (ratios larger than 4,000). For 2004–2005, the mean ratio of 1–3 Hz/10–20 Hz pseudo energy was 140 (standard deviation 340); for 2008–2009 this ratio was 31 (standard deviation of 80).

[16] Thus, on average, the 1–3 Hz/10–20 Hz energy emission during calving events decreased between the two deployments. Given the large standard deviations it is difficult to say if the ratio change in pseudo energy affects all calving events or just a subgroup. However, using a KS test, we determined that the distribution difference of pseudo energy ratios for the two deployments is statistically significant at a 99.9% confidence interval.

[17] The seismic record of the largest calving events (1–3 Hz detection duration longer than 500 seconds) exhibits similar statistical characteristics. Seven of the eight largest 2004–2005 calving events have pseudo energy ratios greater than five, with 24 being the maximum. In contrast, eight of the nine largest detected calving events in 2008–2009 had pseudo energy ratios smaller than three.

5. Discussion and Conclusions

[18] Our analysis demonstrates changes in seismic signals associated with the grounded to floating transition at Columbia Glacier. Event detections in both the 1–3 Hz and 10–20 Hz frequency band decreased after flotation, in accordance with visual and photogrammetric observations that calving occurs less frequently but on a much larger scale after flotation. Prolonged periods of 1–3 Hz seismicity are less common after flotation (Figure 2a), and the 1–3 Hz/10–20 Hz energy ratio decreases during individual calving events. We interpret the latter observation as a mechanical change in fracture processes during iceberg detachment, assuming that both 1–3 Hz and 10–20 Hz waves travel along the same paths and that higher frequencies are more prone to attenuation. Specifically, we consider the conceptual model that hydraulic fracturing forces a substantial portion of grounded calving [*O'Neel and Pfeffer*, 2007]. According to this mechanism pressurized basal water opens and extends fractures into ice. Under floating conditions, overpressured water cannot exist at the terminus base, and seismic events sourced by basal hydraulic fracture should only locate to grounded portions of the glacier.

[19] This study elucidates some fundamental differences between grounded tidewater and ice shelf calving. For example, on the Ross Ice Shelf significant calving events occur infrequently (years to decades) via rift extension over large portions of the shelf width [*Jacobs et al.*, 1986; *Lazara et al.*, 1999]. Though located in a different glaciological setting, Columbia Glacier has qualitatively shifted towards a characteristic calving style of ice shelves since its terminus came afloat.

[20] Rift formation plays a crucial role in iceberg calving from floating termini, and appears to be important in the current mode of calving at Columbia Glacier (see auxiliary material). We suggest that constant periodic bending due to tidal uplift [e.g., *Reeh et al.*, 2003], ocean gravity waves [e.g., *Kristensen et al.*, 1982; *MacAyeal et al.*, 2006] and normal oscillations of the water masses within the fjord "seiches" [*Miles*, 1974] weaken the ice tongue and induce rift formation near the grounding line. Ample "starter-cracks" are available along the highly crevassed surface of Columbia Glacier to initiate rifting. We consider it likely that pervasive rifts are driven into the ice as far back as the grounding line, where longitudinal strain rates are expected to be high [*Greve and Blatter*, 2009]. On the other hand, in the case of a grounded tidewater glacier, longitudinal stretching is highest much closer to the terminus. This may explain the absence of large rifts and the relatively small but frequent calving events prior to the flotation of Columbia Glacier's terminus. Detailed mechanical modeling is required to support these conjectures.

[21] Our data and interpretation support a calving rule where iceberg production is dependent on near-terminus geometry and flow dynamics [*Benn et al.*, 2007; *Alley et al.*, 2008] and can be weakly or discontinuously sensitive to external mechanical forcings (e.g., tides). Stable floating termini are normally observed in polar settings (e.g., Antarctica and Greenland); Columbia Glacier may represent the only known example of a sustained flotation of a temperate glacier terminus. The floating region results from a unique combination of surface and bed geometry (Figure 1). During short-term terminus advances, the terminus protrudes into deeper water quickly approaching flotation. The observation that rift-induced calving events immediately disintegrate, rather than forming tabular icebergs suggests that the highly fractured floating tongue is unstable over decadal or longer time scales.

[22] When the terminus is grounded, the far-field stress state is characteristically variable; nearly constant, energetic calving (Figure S2) results from fracture propagation between networks of exiting damage. Upon flotation, the stress field relaxes and unifies (the basal shear traction becomes very small). With stress perturbations existing only at the margins, material damage can be sustained at a much higher level. Damage concentrates near points of weakness promoting large-scale crevasse (rift) formation. Calving is no longer triggered by the propagation of large fractures, but by small-scale linking between existing damage, as evidenced by the reduction in seismic energy transmission (Figure S2) and larger iceberg sizes.

[23] In conclusion, our study presents visual and seismologic evidence for a mechanical change in calving at Columbia Glacier as the terminus went afloat. The observation of a floating tongue at a temperate tidewater glacier fills a critical gap in the continuum of mechanical process describing the transition of the basal boundary condition from grounded to floating. The results of this study suggest that the flotation criterion distinguishes between ice shelf and tidewater calving styles independent of external mechanical forcing. In order to reliably predict future sea-level variations, ice sheet models must incorporate both calving styles and the possibility of a transition in regime, as observed on Columbia Glacier.

[24] **Acknowledgments.** This work was supported by NSF ANT-0739769 and IPY-0732726. Jason Amundson and an anonymous reviewer provided insightful comments. The Extreme Ice Survey supported time-lapse photography campaigns from 2006 to 2010. Thanks to M. Kennedy for rendering the video in short order. Richard Boaz provided valuable assistance with the installation and set up of the PQLX software.

References

Alley, R. B., H. J. Horgan, I. Joughin, K. M. Cuffey, T. K. Dupont, B. R. Parizek, S. Anandakrishnan, and J. Bassis (2008), A simple law for ice-shelf calving, *Science*, *322*(5906), 1344, doi:10.1126/science.1162543.

Amundson, J., M. Truffer, M. P. Lüthi, M. Fahnestock, M. West, and R. J. Motyka (2008), Glacier, fjord, and seismic response to recent large calving events, Jakobshavn Isbrae, Greenland, *Geophys. Res. Lett.*, *35*, L22501, doi:10.1029/2008GL035281.

Amundson, J. M., M. Fahnestock, M. Truffer, J. Brown, M. P. Lüthi, and R. J. Motyka (2010), Ice mélange dynamics and implications for terminus stability, Jaobshavn Isbrae, Greenland, *J. Geophys. Res.*, *115*, F01005, doi:10.1029/2009JF001405.

Aster, R. C., D. E. McNamara, and P. D. Bromirski (2008), Multidecadal climate-induced variability in microseims, *Seismol. Res. Lett.*, *79*(2), 194–202, doi:10.1785/gssrl.79.2.194.

Benn, D. I., R. J. Hulton, and R. H. Mottram (2007), "Calving laws, " "sliding laws" and the stability of tidewater glaciers, *Ann. Glaciol.*, *46*, 123–130, doi:10.3189/172756407782871161.

Greve, R., and H. Blatter (2009), *Dynamics of Ice Sheets and Glaciers*, Springer, New York.

Jacobs, S. S., D. R. MacAyeal, and J. L. Ardai Jr. (1986), The recent advance of the Ross Ice Shelf, Antarctica, *J. Glaciol.*, *32*, 464–474.

Kristensen, M., V. A. Squire, and S. C. Moore (1982), Tabular icebergs in ocean waves, *Nature*, *297*(5868), 669–671, doi:10.1038/297669a0.

Lazara, M. A., L. C. Jezek, T. A. Scambos, D. R. MacAyeal, and C. J. van der Veen (1999), On the recent calving of icebergs from the Ross Ice Shelf, *Polar Geogr.*, *23*(3), 201–212, doi:10.1080/10889379909377676.

Longuet-Higgins, M. S. (1950), A theory of the origin of microseisms, *Philos. Trans. R. Soc. A*, *243*, 1–35, doi:10.1098/rsta.1950.0012.

MacAyeal, D. R., et al. (2006), Transoceanic wave propagation links iceberg calving margins of Antarctica with storms in tropics and Northern Hemisphere, *Geophys. Res. Lett.*, *33*, L17502, doi:10.1029/2006GL027235.

MacAyeal, D. R., E. A. Okal, R. C. Aster, and J. N. Bassis (2008), Seismic and hydroacoustic tremor generated by colliding icebergs, *J. Geophys. Res.*, *113*, F03011, doi:10.1029/2008JF001005.

McNamara, D. E., and R. P. Buland (2004), Ambient noise levels in the continental United States, *Bull. Seismol. Soc. Am.*, *94*(4), 1517–1527, doi:10.1785/012003001.

Meier, M. F., and A. Post (1987), Fast tidewater glaciers, *J. Geophys. Res.*, *92*, 9051–9058, doi:10.1029/JB092iB09p09051.

Meier, M. F., M. B. Dyurgerov, U. K. Rick, S. O'Neel, W. T. Pfeffer, R. S. Anderson, S. P. Anderson, and A. F. Glazovsky (2007), Glaciers dominate eustatic sea-level rise in the 21st Century, *Science*, *317*(1064), 1064–1067, doi:10.1126/science.1143906.

Miles, J. W. (1974), Harbor seiching, *Annu. Rev. Fluid Mech.*, *6*, 17–33, doi:10.1146/annurev.fl.06.010174.000313.

Neave, K. G., and J. C. Savage (1970), Icequakes on the Athabasca glacier, *J. Geophys. Res.*, *75*, 1351–1362, doi:10.1029/JB075i008p01351.

O'Neel, S., and W. T. Pfeffer (2007), Source mechanisms for monochromatic icequakes produced during iceberg calving at Columbia Glacier, AK, *Geophys. Res. Lett.*, *34*, L22502, doi:10.1029/2007GL031370.

O'Neel, S., W. T. Pfeffer, R. Krimmel, and M. Meier (2005), Evolving force balance at Columbia Glacier, Alaska, during its rapid retreat, *J. Geophys. Res.*, *110*, F03012, doi:10.1029/2005JF000292.

O'Neel, S., H. Marshall, D. McNamara, and W. T. Pfeffer (2007), Seismic detection and analysis of icequakes at Columbia Glacier, Alaska, *J. Geophys. Res.*, *112*, F03S23, doi:10.1029/2006JF000595.

Qamar, A. (1988), Calving icebergs: A source of low-frequency seismic signals from Columbia Glacier, Alaska, *J. Geophys. Res.*, *93*, 6615–6623, doi:10.1029/JB093iB06p06615.

Reeh, N., E. L. Christensen, C. Mayer, and O. B. Olesen (2003), Tidal bending of glaciers: a linear viscoelastic approach, *Ann. Glaciol.*, *37*, 83–89, doi:10.3189/172756403781815663.

Rignot, E., J. L. Bamber, M. R. van den Broeke, C. Davies, Y. Li, W. J. van de Berg, and E. van Meigaard (2008), Recent Antarctic ice mass loss from radar interferometry and regional climate modeling, *Nat. Geosci.*, *1*, 106–110, doi:10.1038/ngeo102.

van den Broeke, M., J. Bamber, J. Ettema, E. Rignot, E. Schrama, W. J. van de Berg, E. van Meijgaard, I. Velicogna, and B. Wouters (2009), Partitioning recent Greenland mass loss, *Science*, *326*(5955), 984–986, doi:10.1126/science.1178176.

Walter, F., J. F. Clinton, N. Deichmann, D. S. Dreger, S. E. Minson, and M. Funk (2009), Moment tensor inversions of icequakes on Gornergletscher, Switzerland, *Bull. Seismol. Soc. Am.*, *99*(2A), 852–870, doi:10.1785/0120080110.

J. N. Bassis, Department of Geological Sciences, University of Michigan, Ann Arbor, MI 48109-2143, USA.

H. A. Fricker and F. Walter, Institute of Geophysics and Planetary Physics, University of California, San Diego, La Jolla, CA 92093-0225, USA.

D. McNamara, U.S. Geological Survey, Golden, CO 80401, USA.

S. O'Neel, U.S. Geological Survey, Alaska Science Center, Anchorage, AK 99775, USA.

W. T. Pfeffer, Institute of Arctic and Alpine Research, University of Colorado at Boulder, Boulder, CO 80309-0450, USA.